

Three-dimensional stiff cellular structures with negative Poisson's ratio

Dong Li^a, Jie Ma^a, Liang Dong^b and Roderic S. Lakes^c

^a *College of Sciences, Northeastern University, Shenyang 110819, PR China*

^b *Materials Science and Engineering, University of Virginia, Charlottesville, VA 22904, USA*

^c *Department of Engineering Physics, University of Wisconsin, Madison, WI 53706-1687, USA*

Preprint

Li, D., Ma, J., Dong, L. Lakes, R. S., "Three-dimensional stiff cellular structures with negative Poisson's ratio" *Physica Status Solidi B*. 254, (12) 1600785, 5 pages Dec. (2017).

Abstract:

In this paper, a novel three-dimensional (3D) cellular structure with negative Poisson's ratio was designed by alternating cuboid surface indents on the vertical ribs of the unit cells. The Poisson's ratio and Young's modulus of structures with different geometric parameters were determined using the finite element method (FEM) as a function of these parameters. Samples with identical geometric variables were fabricated via 3D printing, and their through-thickness direction Poisson's ratios were measured and compared with simulation results. Results showed that the Poisson's ratio of the 3D cellular structures can be tuned from positive to negative and can reach a minimal value of -0.953. Good agreement was found between the experimental results and the simulation. This lattice structure is considerably stiffer than re-entrant negative Poisson's ratio foam with the same solid phase. The design concept developed here can be optimized for specific applications via geometric parameters manipulation.

Keywords: Three-dimensional cellular structural; Negative Poisson's ratio; Finite element method (FEM); Elastic properties; 3D printing

1. INTRODUCTION

Cellular solids are widely used for many structural applications due to the low weight and high energy absorption capability [1]. 2D cellular solids can exhibit a negative Poisson's ratio if the cells have an inverted bow-tie shape [2, 3]. Negative Poisson's ratio gives rise to a predicted increase in some material properties including such as flexural rigidity and plane strain fracture toughness [4].

Negative Poisson's ratio polyurethane foam with re-entrant structure was first developed as a 3D material by Lakes in 1987 [5]. Subsequently, many kinds of designed cellular materials with negative Poisson's ratio were fabricated in both 2D [6-11] and 3D structures [12-14]. However, most 2D cellular structures that exhibit negative Poisson's ratio were due to the cells with inverted bow-tie shape. Negative Poisson's ratio behavior has also been observed experimentally in polymer gels near their phase transitions [15, 16], in orthorhombic alloy in a set of planes [17], and in ferroelastic ceramic [18] near a temperature dependent phase transformation and in InSn alloy [19] near a composition dependent morphotropic phase transformations.

A 2D negative Poisson's ratio structure without re-entrant cells has been reported in our recent work [20]. In the present study, a 3D cellular structure with alternating cuboid surface indents on the vertical ribs is proposed. The Poisson's ratio and Young's modulus of the proposed 3D model were studied via FEM simulations. Samples with identical geometric variables were fabricated via 3D printing, and good agreement was found between the experimental results and the simulation. The model we designed is stiffer than bend dominated structures such as honeycomb in plane and open cell foams. The design concept developed here can be optimized for specific applications via geometric parameters manipulation.

2. FEM SIMULATION

The Poisson's ratio of the designed 3D re-entrant structure has been studied using the commercial finite element software ANSYS. Schematic drawings of the unit cell and the cellular structure model made from periodically packing of the unit cells are shown in Fig. 1(a, b). The schematic drawing of the designed unit cell structure viewed in the x-z plane is shown in Fig. 1c. The length and height of the crossbeam were l and h_0 . The thickness of rib and crossbeam was t which is shown in Fig. 1(a). The distance between the two central axes of crossbeams was denoted as H_1 . It was assumed that $L_0=H_0$, $h_0=l_0=t$, $H_0/h_0=7$ and $L_0/l_0=7$; h_1/h_0 was set to vary from 1.2 to 2.8 with an incremental step of 0.2, and l_1/l_0 was set to vary from 0.1 to 0.9 with an incremental step of 0.1. Free meshes of 368313 elements (Solid 186, 20 nodes) were used to simulate 3D models. The two bottom crossbeams in the middle of the model shown in Fig. 1(b) was fixed, with all degrees of freedom being constrained; the other eight bottom crossbeams near the edges of the model were constrained only in the Z direction. Maximum tensile strain was set to be 0.1% and applied on the top crossbeams of the model along the vertical direction(Z direction). A Poisson's ratio of 0.39 and a Young's modulus of 2.2GPa for the parent material were used for the analysis. These values correspond to those of the ABS polymer used to make 3D printed embodiments of the structure.

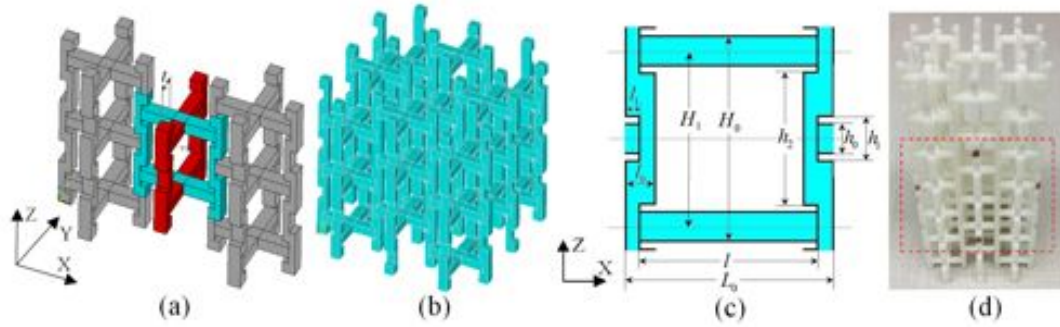


Fig. 1 (a) the ANSYS model of the designed 3D unit cell (in blue and red); (b) the ANSYS model of the designed 3D cellular structure made from periodically packing the unit cells shown in (a); (c) Schematic drawing of the designed unit cell structure viewed in the x-z plane (the part in blue in (a) is shown in detail in "(c)"); (d) a 3D sample fabricated by 3D printing (the part highlighted in the dashed box has an identical size to the FE model shown in (b)).

3. EXPERIMENT

A Stratasys Dimension Elite 3D printer was used to fabricate samples using ABS as the parent material, Fig. 1(d). The size of 3D samples was 100mm in height and 47.5mm for the side length. Samples were compressively loaded in the Z direction using a universal testing machine (MTS Q-Test/5) with a testing speed of 0.01mm/sec. Photographic images were captured simultaneously. Images of the four points marked in red in Fig. 1(d) were taken using a digital camera at each 0.1% normal strain increment. For each normal strain increment, an average of 3 independent measurements were used to calculate the transverse strain which was later used to determine the specimen Poisson's ratio ν at that specific normal strain. To minimize the end effect due to friction between the sample surfaces and the instrument platens, only displacements in the middle part of the specimen were monitored(the size of the middle part of the specimen are identical to that in the FE model shown in Figure 1(b)).

4. RESULTS AND DISCUSSION

4.1. Simulation results

Poisson's ratio is defined as the ratio of the transverse contraction strain to the longitudinal extension strain in the direction of stretching force as:

$$\nu = -\frac{\varepsilon_X}{\varepsilon_Z} \quad (1)$$

where, ν is Poisson's ratio, ε_X and ε_Z are the transverse contraction strain and longitudinal extension strain, respectively. Poisson's ratio in Eq. 1 is the same in all directions only for isotropic materials. In the present model, the 3D structure possesses tetragonal symmetry in which Poisson's ratio depends on direction; ν_{zx} (or ν_{zy}) was studied. It was found that transverse strains ε_X and ε_Y differed by less than 5% for the same axial (z) load; this is consistent with the tetragonal structural symmetry. Therefore, only ν_{zx} was studied further in the following.

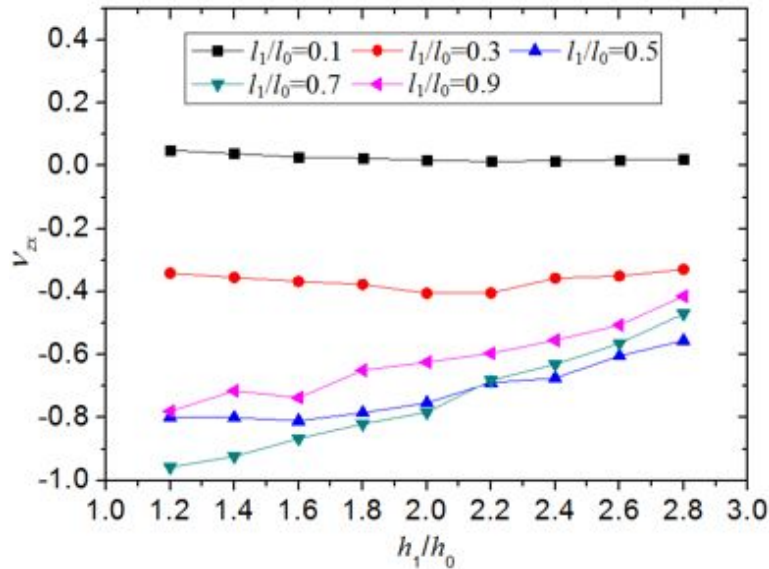


Fig. 2 The relationship between the Poisson's ratio (ν_{zx}) of the designed 3D cellular structure and h_1/h_0 as a function of l_1/l_0 .

Fig. 2 shows the relationship between the Poisson's ratio (ν_{zx}) of the designed 3D cellular structure and the h_1/h_0 ratio (from 1.2 to 2.8) when the l_1/l_0 ratio is varied from 0.1 to 0.9. From Fig.2(a) we can see that the Poisson's ratio of the cellular structure increased with an increasing h_1/h_0 when $l_1/l_0=0.9, 0.7$ and 0.5 , but was insensitive to h_1/h_0 when $l_1/l_0=0.3$ and 0.1 . When $l_1/l_0=0.1$, the Poisson's ratio was close to zero. The near zero Poisson's ratio allows the structure to be readily deformed into a cylinder to provide a core for curved sandwich panels used for aircraft and other applications. A minimum Poisson's ratio, -0.958 , of the 3D cellular structure was achieved when $h_1/h_0=1.2$ and $l_1/l_0=0.7$.

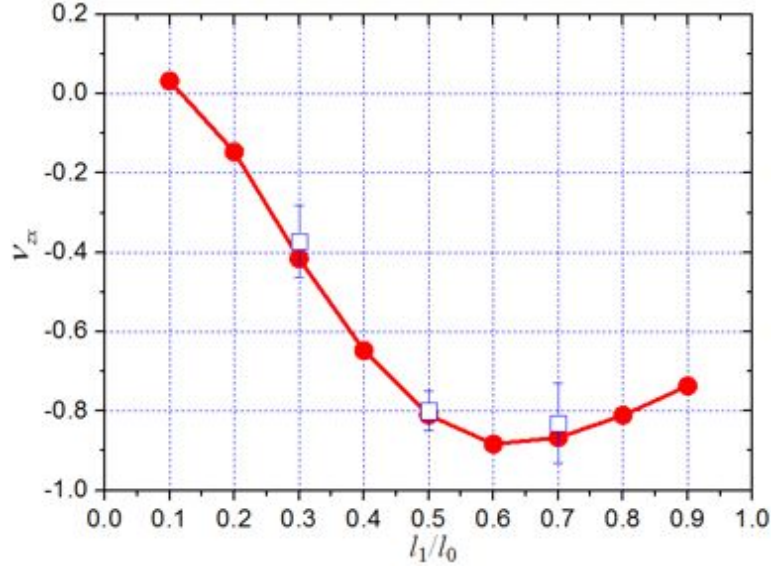


Fig. 3 The relationship between the Poisson's ratio (v_{zx}) of the designed 3D cellular structure and the l_1/l_0 ratio when $h_1/h_0=2$. The experimental data are represented by (\square).

The relationship between the Poisson's ratio (v_{zx}) of the cellular structures and the l_1/l_0 ratio when $h_1/h_0=2$ is shown in Fig. 3. From Fig. 3 we can see that the Poisson's ratio of the 3D cellular structure decreased rapidly with an increasing l_1/l_0 ratio from 0.1 to 0.6, and then slowly increased with an increasing l_1/l_0 ratio from 0.6 to 0.9. The simulation results have shown that the Poisson's ratio of the cellular structure is tunable from +0.032 to -0.883 with an appropriate combination of geometric parameters when $h_1/h_0=2$. The wide tunable range of the Poisson's ratio is of interest for practical designs.

4.2. Experimental results

3D Samples with geometric variables of $h_1/h_0=2.0$ and $l_1/l_0=0.3, 0.5$ and 0.7 were manufactured by 3D printing using ABS as the parent material. For each type of geometric combination (h_1/h_0 and l_1/l_0), three specimens were made from which the Poisson's ratios were measured and their average and the standard deviation were calculated. The measured Poisson's ratios of the samples were plotted to compare with the simulation results, as shown in Fig. 3. The measured Poisson's ratios of the 3D model were -0.372 ± 0.09 when $l_1/l_0=0.3$, -0.8 ± 0.05 when $l_1/l_0=0.5$, and -0.83 ± 0.1 when $l_1/l_0=0.7$. It can be seen that the measurements are in good agreement with the simulation results.

4.3 Stiffness analysis

For low density cellular structures, the relationship for the modulus is

$$\frac{E^*}{E_s} = C \cdot \left(\frac{\rho^*}{\rho_s} \right)^n \quad (2)$$

in which E^* , E_s are the homogenized Young's modulus of the cellular structures and the Young's modulus of the parent material used for making the cellular structures, respectively; C is a geometrical coefficient which includes all of the geometric constants of proportionality; ρ^* and ρ_s are the density of the cellular model and the solid from which the cell walls are made, respectively. The value of n generally lies in the range $1 < n < 4$ giving a wide range of possible properties at a given density. For foams with open cells, experimental evidence indicates

that C approximately equals 1 and n equals 2. The value $n=2$ arises in structures that have rib elements that are bend dominated; bend dominated plate elements that govern in plane behavior of honeycomb and in true closed cell foams correspond to $n=3$. Structures with stretch dominated elements correspond to $n=1$. For the models presented here, the homogenized Young's modulus of the unit cell (in Fig. 1) was obtained using FEM, and the relationship between the relative density and geometric parameters was obtained according to the simple geometry of the unit cell.

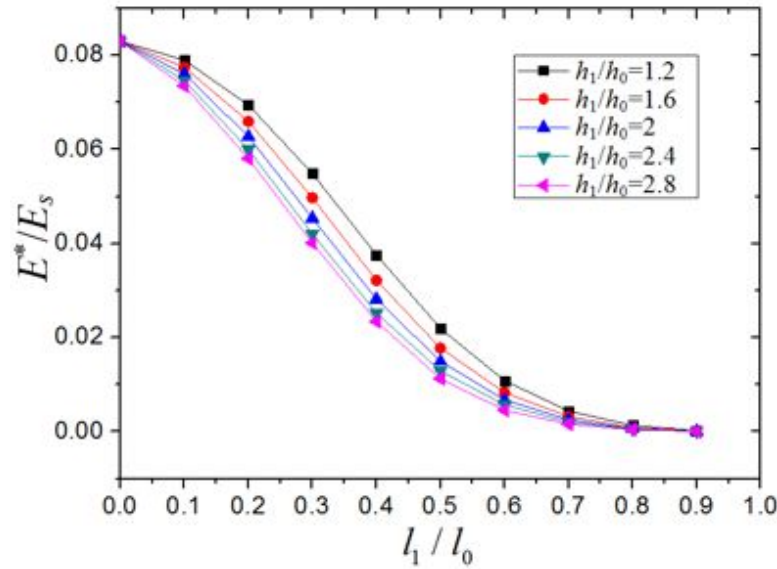


Fig. 4 The relationship between E^*/E_s and l_1/l_0 ratio of the designed 3D cellular structure with different h_1/h_0 . (-■-), (-□-), (-▲-), (-▼-) and (-◄-) represent $h_1/h_0=1.2, 1.6, 2.0, 2.4$ and 2.8 , respectively.

Fig. 4 shows the relationship between E^*/E_s of the designed 3D cellular structure and the l_1/l_0 ratio when the h_1/h_0 ratio is varied from 1.2 to 2.8. From Fig. 4(a) we can see that the E^*/E_s ratio exhibited a similar behavior for different h_1/h_0 ratio: for any specific h_1/h_0 ratio, the E^*/E_s ratio decreased slowly with an increasing l_1/l_0 ratio when l_1/l_0 is less than 0.1, and then decreased rapidly with an increasing l_1/l_0 ratio from 0.1 to 0.6; after which the E^*/E_s ratio decreased in a much slower rate and approached zero. The maximum value of the E^*/E_s ratio, 0.083, is achieved when $l_1/l_0=0$. Referring to Fig. 3, small values of l_1/l_0 correspond to positive Poisson's ratio. Referring to Fig. 1, a value of zero eliminates the indents.

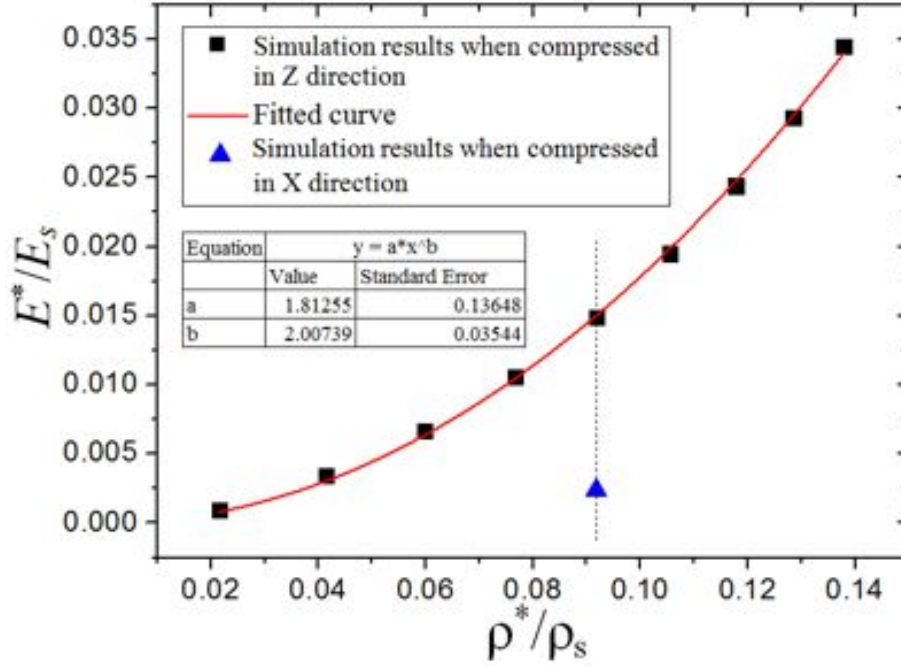


Fig. 5. The relationship between E^*/E_s and ρ^*/ρ_s of the cellular structure when $h_1/h_0=2.0$ and $l_1/l_0=0.5$. (■) represents the simulation results, and (—) is the fitted curve for the simulation results.

Fig. 5 shows the relationship between E^*/E_s and ρ^*/ρ_s of the cellular structure when $h_1/h_0=2.0$ and $l_1/l_0=0.5$. ρ^*/ρ_s was set to vary from 0.02 to 0.14 by proportionally changing the cross-section side length of ribs and crossbeams of the model. Specifically, we changed parameters l_0 , h_0 , l_1 and t by the same percentage to vary the density and kept parameters h_1 , h_2 , l and H_1 constant. A relative modulus in the transverse direction (compressed in X direction), 0.0024, was also obtained when $\rho^*/\rho_s=0.0918$, as shown in Fig. 5. From Fig. 5 we can see that the relative modulus in the transverse direction was lower than that in vertical direction (compressed in Z direction). Nonlinear fitting was used to curve fit the simulation results for stress in the Z direction (solid squares in Fig. 5) as

$$\frac{E^*}{E_s} = 1.81 \cdot \left(\frac{\rho^*}{\rho_s} \right)^2 \quad (3)$$

From Eq. 3 we can see $n=2$ and $C=1.81$ were determined for the 3D structure we designed. That means this kind of cellular structure was bend dominated ($n=2$). By contrast, normal foams with positive Poisson's ratio have $C=1$. Negative Poisson's ratio foams are a factor 3 to 4 denser than the received foam from which they are made. Their elastic modulus is a factor 3 to 4 less. For a factor 3.5 increase in density a factor 3.5 decrease in modulus, $C=0.023$ for typical negative Poisson's ratio foam. So the present lattice structure is considerably stiffer in relation to density than re-entrant negative Poisson's ratio foam. A simple cubic lattice of straight beams would be even stiffer but would not have a negative Poisson's ratio. The honeycomb with bow-tie inverted hexagons is not as stiff as the honeycomb with regular hexagons.

5. CONCLUSIONS

In this paper, a novel 3D cellular structure achieved by alternating cuboid surface indents on the vertical ribs of the unit cells was designed. and their Poisson's ratios were determined using the finite element method (FEM) as a function of geometric parameters. The simulation results showed that the Poisson's ratio of the 3D cellular

structures was sensitive to the cell dimensional ratio, and the value can be tuned from positive to negative (the minimum can reach -0.953). Samples with identical geometric variables were fabricated via 3D printing, and their Poisson's ratios were measured and compared with the ones from simulation. Excellent agreement was found between the experimental results and the simulation. The stiffness of the lattice structure is considerably greater than that of negative Poisson's ratio re-entrant foam made of the same solid phase. The design concept developed here provides new opportunities for specific applications.

Acknowledgements

This work is supported by “The National Natural Science Foundation of China (11304033) and the Fundamental Research Funds for the Central Universities (N150504006)”. The first author would also like to thank the financial support from the China Scholars Council (File No. 201506085013).

References

- [1] L. J. Gibson, M. F. Ashby (1988) *Cellular Solids: Structure & properties*, Oxford: Pergamon Press
- [2] L. J. Gibson, M. F. Ashby, G. S. Schajer, C. I. Robertson (1982) The mechanics of two dimensional cellular solids, *Proc. Royal Society London*, A382: 25-42
- [3] A.G. Kolpakov (1985) On the determination of the averaged moduli of elastic gridworks, *Prikl. Mat. Mekh* 59, 969-977
- [4] E. A. Friis, R. S. Lakes, J. B. Park, *J. Mat. Sci.*, 23 (1988) 4406-4414.
- [5] Lakes R S, *Science*, 238 (1987) 551.
- [6] Hu H, Silberschmidt V, *J Mater Sci*, 48 (2013) 8493-8500.
- [7] Kaminakis N T, Stavroulakis G E, *Composites: Part B*, 43 (2012) 2655-68.
- [8] Pozniak A A, Smardzewski J, Wojciechowski K W. *Smart Mater Struct*, 22 (2013) 1-11.
- [9] Scarpa F, Blain S, Lew T, Perrott D, Ruzzene M, Yates J R, *Compos A*, 38 (2007) 280-289.
- [10] Wojciechowski K W, *Physics Letters A*, 137 (1989) 60-64.
- [11] Grima J N and Evans K E, *J. Mater. Sci. Lett.*, 19 (2000) 1563-1565.
- [12] Li D, Dong L, Lakes R S, *Materials Letters*, 164 (2016) 456-459.
- [13] Buckmann T, Schittny R, Thiel M, Kadic M, Milton G W, Wegener M, *New J Phys*, 16 (2014)
- [14] Li D, Dong L, Lakes R S, *Phys. Status Solidi B*, 250 (2013) 1983-1987.
- [15] S. Hirotsu, *J. Chem. Phys.* 94 (1991) 3949.
- [16] S. Hirotsu, *Macromolecules* 23 903 (1990).
- [17] M. Rovati, *Scripta. Mater.* 48 (2003) 235-240.
- [18] L. Dong, D.S. Stone, R.S. Lakes, *Philos. Mag. Letts.* 90 (2010) 23-33
- [19] Li, D., Jaglinski, T. M., Stone, D. S. and Lakes, R. S., *Appl. Phys. Lett.* 101(2012) 251903
- [20] Dong Li, Jie Ma, Liang Dong, Roderic S. Lakes, Stiff square structure with a negative Poisson's ratio, *Materials Letters* (2016) doi: <http://dx.doi.org/10.1016/j.matlet.2016.11.036>.